

# Neural Crest Origin of Perivascular Mesenchyme in the Adult Thymus<sup>1</sup>

Susanna M. Müller,<sup>2\*</sup> Claus C. Stolt,<sup>2†</sup> Grzegorz Terszowski,<sup>2\*</sup> Carmen Blum,<sup>\*</sup> Takashi Amagai,<sup>‡</sup> Nicoletta Kessar,<sup>§</sup> Palma Iannarelli,<sup>§</sup> William D. Richardson,<sup>§</sup> Michael Wegner,<sup>†</sup> and Hans-Reimer Rodewald<sup>3\*</sup>

The endodermal epithelial thymus anlage develops in tight association with neural crest (NC)-derived mesenchyme. This epithelial-NC interaction is crucial for thymus development, but it is not known how NC supports thymus development or whether NC cells or their progeny make any significant contribution to the adult thymus. By nude mouse blastocyst complementation and by cell surface phenotype, we could previously separate thymus stroma into *Foxn1*-dependent epithelial cells and a *Foxn1*-independent mesenchymal cell population. These mesenchymal cells expressed vascular endothelial growth factor-A, and contributed to thymus vascularization. These data suggested a physical or functional association with thymic blood vessels, but the origin, location in the thymus, and function of these stromal cells remained unknown. Using a transgenic mouse expressing Cre recombinase in premigratory NC (Sox10-Cre), we have now fate-mapped the majority of these adult mesenchymal cells to a NC origin. NC-derived cells represent tightly vessel-associated pericytes that are sandwiched between endothelium and epithelium along the entire thymus vasculature. The ontogenetic, phenotypic, and positional definition of this distinct perivascular mesenchymal compartment provides a cellular basis for the role of NC in thymus development and possibly maintenance, and might be useful to address properties of the endothelial-epithelial barrier in the adult thymus. *The Journal of Immunology*, 2008, 180: 5344–5351.

The neural crest (NC)<sup>4</sup> generates highly migratory cells that contribute in development to diverse cell types, including neurons and glia and connective tissue such as bone and smooth muscle (1–3). During thymus organogenesis, NC-derived mesenchymal cells colonize the branchial arches and pouches and surround the thymic epithelial anlage (4). There is ample evidence from in vivo and in vitro experiments that this contact of thymus epithelium with embryonic NC-mesenchyme (NC-Mes) is functionally important for thymus development. Ablation of cephalic NC in birds prevents contributions of NC-Mes to the thymus. Under these conditions, thymus development is delayed and the thymus remains small and poorly functional (5) (reviewed in Refs. 6–9). A requirement for mesenchymal-epithelial contact for thymus growth has also been demonstrated in thymus

organ cultures (10–12) (reviewed in Ref. 7) and in thymus grafts assembled from thymic epithelium in the presence or absence of mesenchyme (13).

Although the importance of at least a transient contribution of NC-derived cells to the embryonic thymus is well established, it has remained enigmatic to what extent NC-derived cells make a long-lasting contribution to the adult thymus. For instance, it is not clear whether embryonic NC-Mes and adult thymus mesenchyme share a precursor-product relationship (reviewed in Refs. 9, 14, and 15). An additional complication arises from the fact that thymic mesenchymal cells are of diverse nature and functions. Mesenchymal stromal cells not only include connective tissue-forming cells required for the capsule and the septae, but also endothelial cells, perivascular cells, and plain thymic fibroblasts that are abundantly present in the thymus. Thymic mesenchymal structures can be recognized by mAb ERTR-7 (16) and MTS15 (17), but very little information is available on phenotypes, heterogeneity, turnover, and, most of all, origin and thymus-specific functions of these cell types.

Because NC is the major source of thymic mesenchyme in ontogeny, it is conceivable that some or all of the adult mesenchymal cells are of NC origin. In contrast to this original view (4) (reviewed in Refs. 9 and 15), several more recent studies came to the conclusion that very few, if any, NC-derived cells are present in the adult thymus (14, 18, 19). This assumption was based on the absence of cells in the adult thymus marked by Cre-dependent activation of a Rosa-LacZ reporter locus in genetic fate-mapping experiments. In mice that express Cre-recombinase under the control of NC-specific genes, NC derivatives are indelibly labeled. In two such NC-Cre lines, Wnt1-Cre (14, 18) and protein zero (P0)-Cre (19), a layer of labeled cells surrounded the embryonic thymus, and represented by flow cytometry as many as 30% of all stromal cells on E13.5 (19). This confirmed the substantial and early participation of NC in thymus development. Surprisingly, however, the overall contribution of labeled cells rapidly declined

\*Institute for Immunology, University of Ulm, Ulm, Germany; †Institute for Biochemistry, University Erlangen-Nürnberg, Erlangen, Germany; ‡Department of Immunology and Microbiology, Meiji University of Oriental Medicine, Hiyoshi-cho, Funai-gun, Kyoto, Japan; and §Wolfson Institute for Biomedical Research and Department of Biology, University College London, London, United Kingdom

Received for publication November 13, 2007. Accepted for publication February 6, 2008.

The costs of publication of this article were defrayed in part by the payment of page charges. This article must therefore be hereby marked *advertisement* in accordance with 18 U.S.C. Section 1734 solely to indicate this fact.

<sup>1</sup> H.-R.R. was supported by grants from the Deutsche Forschungsgemeinschaft (SFB 497-B5 and Klinische Forschergruppe 142-P8).

<sup>2</sup> S.M.M., C.C.S., and G.T. made equal contributions to this study.

<sup>3</sup> Address correspondence and reprint requests to Dr. Hans-Reimer Rodewald, Institute for Immunology, University of Ulm, D-89081 Ulm. E-mail address: hans-reimer.rodewald@uni-ulm.de

<sup>4</sup> Abbreviations used in this paper: NC, neural crest; 3<sup>rd</sup> pp, third pharyngeal pouch; *Cnn1*, *Calponin1*; cTEC, cortical thymus epithelial cell; E11.5, embryonic day 11.5; Fgf, fibroblast growth factor; mTEC, medullary thymus epithelial cell; NC-Mes, NC mesenchyme; P0, protein zero; Pdgfr, platelet-derived growth factor receptor; Scf, stem cell factor;  $\alpha$ SMA,  $\alpha$ -smooth muscle actin; TEC, thymus epithelial cell; Vegf-A, vascular endothelial growth factor; wt, wild type; YFP, yellow fluorescent protein.

in the fetal thymus until, in the newborn and adult thymus, NC-derived cells appeared to be absent, or almost so. These data suggested that NC mesenchyme plays no role, or a very minor role in the postnatal organ (14, 18, 19) (reviewed in Refs. 9 and 15). From a technical point of view, this conclusion depended on the sensitivity of the detection of Cre-driven expression of Rosa-LacZ in adult thymus stromal cells.

In tetraparental chimeras between wild-type (wt) and nude mouse parents, the Foxn1-dependent and Foxn1-independent stromal cell compartments have been dissected genetically (20–22). Using nude blastocyst complementation, the key vascular endothelial growth factor (Vegf)-A has been ablated in thymus epithelium, but not in thymus mesenchyme (22). In these experiments, we identified by cell surface phenotype a distinct mesenchymal population, coined cortical mesenchyme, that arose selectively from the *Foxn1<sup>nu/nu</sup>* origin, that expressed Vegf-A, and that contributed to thymus vascularization in the absence of epithelial Vegf-A. However, without further information regarding the intrathymic location and possible function of these cells, or whether they represent generic thymus fibroblasts (17), these mesenchymal cells remained enigmatic (23). Using Sox10-Cre-driven lineage tracing, we now report that this mesenchymal cell population originates from the NC and, extending the original findings in bird embryos (4), represents perivascular mesenchyme lining the entire adult thymic vasculature. Hence, these cells represent the elusive structural component of the NC in the adult thymus. Finally, the high percentage of NC ancestry labeling in this pericyte compartment suggests very little, if any, replacement of these cells by non-NC-derived mesenchyme in the steady-state thymus.

## Materials and Methods

### Mice

Sox10-Cre Rosa-yellow fluorescent protein (YFP) mice were bred from Sox10-Cre mice (2) and Rosa-YFP reporter mice (24). Littermates (Sox10-wt Rosa-wt) were used as negative controls. Germline-deleted Rosa-YFP mice were a gift from T. Boehm (Freiburg, Germany). For analysis of embryonic tissues, mice were timed-mated counting the morning of the plug as day 0.5. All animal studies have been reviewed and approved by the institutional review committee (Regierungspräsidium Tübingen).

### Immunofluorescence analysis of tissue sections

Thymi were fixed in 4% paraformaldehyde for 2 h on ice, washed in PBS, kept in 30% sucrose for 40 h, and embedded in OCT on dry ice. Cryosections (5  $\mu$ m) were rehydrated, and endogenous biotin was blocked by endogenous biotin-blocking kit (Molecular Probes). Staining was conducted in PBS, 10% normal goat serum, 1% BSA, and 0.2% Tween 20 using the following reagents: Cy3-conjugated anti- $\alpha$  smooth muscle actin (SMA) (clone 1A4, 1:200; Sigma-Aldrich), polyclonal rabbit anti-GFP (1:1000; Molecular Probes), Alexa-488-conjugated goat anti-rabbit IgG (1:500; Molecular Probes), Cy3.5-conjugated anti-pan-cytokeratin (cl. C11, self labeled, 1:10; Neomarkers), biotin-conjugated anti-CD31 (cl. MEC13.3, 1:100; BD Pharmingen), PE-labeled Ly51 (clone BP1, 1:200), Alexa-647-conjugated streptavidin (1:400; Molecular Probes), polyclonal rabbit anti-Foxn1 (25), and Alexa-647-conjugated donkey anti-rabbit IgG (1:400; Molecular Probes). Sections were analyzed on an Axioskop (Zeiss) with Openlab software (Improvision), or on a spectral imaging confocal laser scanning system (Nikon C1si, Nikon Imaging Center, University of Heidelberg) with Nikon EZ-C1 software.

### Whole-mount embryos

Embryonic day 11.5 (E11.5) embryos were fixed in 4% paraformaldehyde for 4 h, washed in PBS, and kept in 30% sucrose overnight. YFP fluorescence was visualized in E11.5 embryos in sucrose using a fluorescence stereomicroscope (MZ16F; Leica Microsystems). A GFP filterset (470/40 nm ex, 525/50 nm em) was used for YFP. Autofluorescence was detected by the DsRed filterset (545/30 nm ex, 620/60 nm em), and red autofluorescence was background subtracted from the YFP signal by Openlab Darkroom software (Improvision). Embryos were subsequently snap frozen in OCT. Sagittal sections of 5  $\mu$ m were cut on a cryostat and stained

with anti-GFP and anti-pan-cytokeratin Ab or with anti-pan-cytokeratin and anti-Foxn1 (all as described above) on serial sections.

### Thymus stromal cell populations

Thymus tissue was enzymatically digested, as described (22). Thymus stromal cells were enriched either by Percoll gradient centrifugation (22) for flow cytometric analysis, or by depletion of CD45-positive cells with magnetic beads (sheep anti-rat IgG; Invitrogen Life Technologies) for subsequent cell sorting. Stromal cell-enriched fractions were stained according to cell surface phenotypes indicated in *Results* using the following reagents: FITC-labeled UEA-1 (1:500; Sigma-Aldrich), biotinylated UEA-1 (1:100; Vector Laboratories), CyChrome-labeled anti-CD45 (clone IM7, 1:200), PE-labeled Ly51 (clone BP1, 1:100), allophycocyanin-labeled anti-CD31 (clone MEC 13.3, 1:500), or biotinylated anti-CD31 (clone MEC 13.3, 1:1000), biotinylated anti-epithelial cell adhesion molecule (clone G8.8, 1:500), and Alexa-647 self-labeled anti-epithelial cell adhesion molecule (clone G8.8, 1:1000) (all from BD Pharmingen). Second-step reagent was streptavidin PE-Cy7 (BD Pharmingen). Cells were analyzed and sorted on a FACS-ARIA instrument equipped with FACS-DIVA software (BD Pharmingen), as reported previously (22). Dead cells were excluded using Sytox Blue (Invitrogen Life Technologies; 1:30,000 from a 1 mM solution in DMSO added to the samples before analysis or sorting).

### RT-PCR

RNA was extracted from  $4 \times 10^4$  sorted cells using RNA-Bee isolation solvent (Tel-Test). The SuperScript First-Strand Synthesis System (Invitrogen Life Technologies) was used for reverse transcription of total RNA. RT-PCR was performed using the following condition: 50 s at 95°C (20 s at 95°C, 20 s at 60°C ( $\alpha$ SMA,  $\beta$ -actin, *Calponin1* (*Cnn1*), fibroblast growth factor 10 (*Fgf10*), *Foxn1*, *Sox10*), or at 65°C (*Ly51*), or at 68°C (stem cell factor (*Scf*), and 30 s at 72°C)  $\times$  35, and 4 min at 72°C. Primers and PCR products were as follows:  $\alpha$ SMA (also termed *Acta2*), DNA product = 476 bp, 5' primer: 5'-CTACTGCCGAGCGTGAGATTGTCC-3' and 3' primer: 5'-AGGGCCCAGCTTCTGCGTATTC-3';  $\beta$ -actin (actin), DNA product = 410 bp, 5' primer: 5'-CATCACTATTGGCAACGAGC-3' and 3' primer: 5'-ACGCAGCTCAGTAACAGTCC-3'; *Cnn1*, DNA product = 406 bp, 5' primer: 5'-AGATTTGAGCCGAGAAAGTTGAGAG-3' and 3' primer: 5'-TAGTAGTTGTGCGGGTGGTGATTGT-3'; *Fgf10*, DNA product = 529 bp, 5' primer: 5'-ACATTGTGCTCAGCCCTTTC-3' and 3' primer: 5'-TTCCATTCAATGCCACATACAT-3'; *Foxn1*, DNA product = 917 bp, 5' primer: 5'-CAGGGCCACTGCACAGCCG-3' and 3' primer: 5'-AGGCTGTCCAGCTCTTCTGG-3'; *Ly51*, DNA product = 418 bp, 5' primer: 5'-TACCGTCATCCGCTACATCTCCTA-3' and 3' primer: 5'-GCTCCCCTCTGCGGTCTGTAAAAC-3'; *Scf*, DNA product = 505 bp, 5' primer: 5'-CTGGCTGCAACAGGGGGTAAAC-3' and 3' primer: 5'-GTCAAAAACCAAGGAGATCTGCGGG-3'; *Sox10*, DNA product = 358 bp, 5' primer: 5'-ACGGCGAGGGCGACGATGAC-3' and 3' primer: 5'-CTTCCGCCCGGAGGTTGGTA-3'. Positive controls were whole thymus cDNA ( $\beta$ -actin, *Fgf10*, *Foxn1*, *Ly51*, *Scf*, *Sox10*) or uterus cDNA ( $\alpha$ SMA, *Cnn1*).

## Results

### *Sox10-Cre-marked tissues include the pharyngeal arch region and the perithymic mesenchyme in the embryo*

To address the long-standing question of whether NC derivatives contribute to the structural components in the adult thymus, we used a fate-mapping strategy that allows the tracing of cells bearing a permanent marker indicative of their NC past. To this end, we made use of a transgenic mouse (Sox10-Cre) expressing Cre recombinase under the control of this NC marker gene (2). *Sox10* is expressed throughout the emerging NC before it becomes restricted to specific NC derivatives. *Sox10* expression is additionally turned on in oligodendrocytes of the CNS (26, 27). In Sox10-Cre mice crossed to a Cre-dependent YFP reporter mouse strain (ROSA26-EYFP (Rosa-YFP)) (24), all progeny of Cre-expressing cells are permanently labeled by YFP expression. By whole-mount fluorescence analysis, YFP was detectable in the ventral neck region on E11.5 in Sox10-Cre Rosa-YFP, but not in wt mice (Fig. 1, A and B). Sectioning of a whole E11.5 embryo revealed, among other NC-derived tissues, dense labeling of the entire pharyngeal

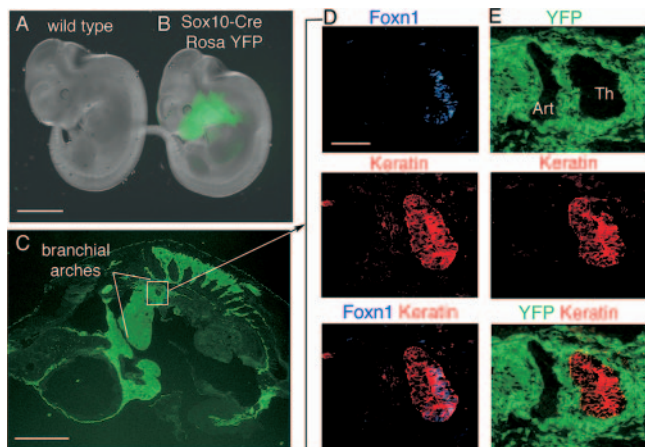


**FIGURE 1.** Sox10-Cre-driven YFP labeling in the embryo, and in the 3<sup>rd</sup> pp. *A* and *B*, Comparison of YFP fluorescence in whole mounts of E11.5-old wt control mice (*A*) and Sox10-Cre Rosa-YFP mice (*B*) shows specific and intensive staining in the area of the pharyngeal arches. Note that, unlike on sections (see *C*), only YFP fluorescence close to the surface (arches) is visible. Scale bar for *A* and *B* corresponds to 1.5 mm. *C*, A section from a whole embryo E11.5 Sox10-Cre Rosa-YFP embryo was stained with an anti-YFP Ab to reveal areas of NC and their derivatives. The entire branchial arch region is labeled (see white lines encompassing the arches). The white frame captures the third pouch region, where the thymus anlage arises. Scale bar for *C* corresponds to 1.0 mm. *D*, Immunofluorescence analyses on E11.5 for expression of Foxn1 vs pan-cytokeratin (keratin) (Foxn1 only (*top*); keratin only (*middle*); overlay of Foxn1 plus keratin (*bottom*)). *E*, Analysis as in *D*, but for expression of YFP vs keratin (YFP only (*top*); keratin only (*middle*); overlay of YFP plus keratin (*bottom*)). Sections are sagittal, and the orientation is cranial on the left, caudal on the right, and dorsal at the top. The thymus anlage, visualized by Foxn1 expression in the caudal part of the pouch, is fully surrounded by YFP<sup>+</sup> cells. Third arch artery (Art) and thymus (Th) anlage are adjacent to each other. Scale bar shown in *D* (*top panel*) corresponds to 80  $\mu$ m and applies to all panels in *D* and *E*.

arch region (Fig. 1C). This expression pattern of Sox10-Cre-labeled tissues was consistent with the known migration pattern and tissue distribution of NC cells (2, 3, 18, 19, 27, 28).

Because the thymus anlage arises from the third pharyngeal pouch (3<sup>rd</sup> pp), this region was analyzed more closely on E11.5 for expression of YFP vs pan-cytokeratin (keratin). Within the keratin<sup>+</sup> structure of the 3<sup>rd</sup> pp, the thymus-committed epithelium was positively identified by Foxn1 expression. In keeping with a previous report (29), Foxn1<sup>+</sup> cells were restricted to the caudal aspect of the 3<sup>rd</sup> pp epithelium (Fig. 1D). The keratin<sup>+</sup> epithelium was fully surrounded by keratin<sup>-</sup>, i.e., nonepithelial cells that homogeneously expressed YFP (Fig. 1E). Hence, Sox10-Cre-driven fate mapping recapitulated the NC origin of nonepithelial cells encapsulating the epithelial thymus anlage in the 3<sup>rd</sup> pp. In contrast, YFP-marked cells were undetectable in the 3<sup>rd</sup> pp epithelium itself. YFP expression in cells immediately adjacent to the developing thymus was consistent with previous tracking of NC derivatives using Wnt1-Cre Rosa-LacZ mice (18), and myelin P0-Cre Rosa-LacZ (19) mice.

#### *Sox10-Cre preferentially marks an adult thymus mesenchymal stromal population previously defined by genetic complementation and phenotype*

Thymic stromal cells comprise lineages of heterogeneous origin. Based solely on phenotype, stromal cells cannot readily be assigned to their origins in ontogeny, which is an important lineage criterion (15). By combining YFP expression with flow cytometric

analysis of stromal cell phenotypes, we searched for NC-specific tagging in the adult thymus. Thymi from Sox10-Cre Rosa-YFP mice were digested to release structural components that were analyzed by flow cytometry for expression of CD45, UEA-1, G8.8, Ly51, and CD31. Viable (Sytox<sup>-</sup>), nonlymphoid (CD45<sup>-</sup>) cells were subdivided into medullary and cortical thymus epithelial cells (TEC), mesenchymal cells, and endothelial cells, according to established cell surface phenotypes (22, 30–33). Cells were first gated as UEA-1<sup>+</sup> or CD31<sup>+</sup> (i.e., UEA-1 and CD31 combined in one color) (Fig. 2A, gate R1), or UEA-1<sup>-</sup>CD31<sup>-</sup>Ly51<sup>+</sup> (Fig. 2A, gate R2). Endothelial cells were identified as CD31<sup>+</sup>Ly51<sup>-</sup>G8.8<sup>-</sup> (Fig. 2B, left gate), medullary TEC (mTEC) were recognized as UEA-1<sup>+</sup>Ly51<sup>-</sup>G8.8<sup>+</sup>CD31<sup>-</sup> (Fig. 2B, right gate), and the UEA-1<sup>-</sup>CD31<sup>-</sup>Ly51<sup>+</sup> population was further separated into G8.8<sup>-</sup> mesenchymal cells (Fig. 2C, left gate) and G8.8<sup>+</sup> cortical TEC (cTEC) (Fig. 2C, right gate).

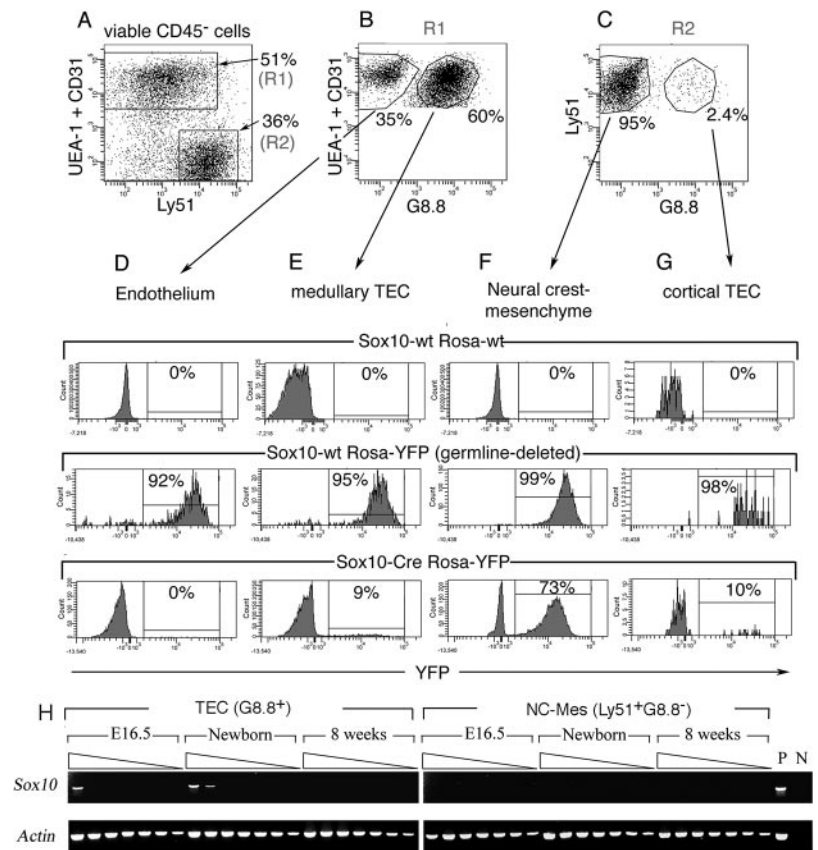
We have previously identified UEA-1<sup>-</sup>CD31<sup>-</sup>Ly51<sup>+</sup>G8.8<sup>-</sup> cells (abbreviated as Ly51<sup>+</sup>G8.8<sup>-</sup> cells below) and termed these cells cortical mesenchyme because they lacked keratin, developed in genetic complementation experiments independently from Foxn1, expressed growth factors such as Fgf10 and Scf, and were identified by flow cytometry based on expression of the cortical marker Ly51 (22). We now demonstrate by fate mapping (see below) that these Ly51<sup>+</sup>G8.8<sup>-</sup> cells are mesenchymal cells of NC origin in the adult thymus. Because developmental ancestry is an unequivocal lineage hallmark, we now designate these cells as thymic NC-Mes.

To determine whether YFP could, in principle, be expressed in all stromal subpopulations, YFP expression was analyzed in germline-deleted Rosa-YFP mice in which YFP expression does not depend on Sox10-Cre expression. Consistent with ubiquitous YFP expression in these mice, between 92 and 99% of the cells in each stromal cell fraction were YFP<sup>+</sup> (Fig. 2, D–G, middle panels), whereas no YFP<sup>+</sup> cells were found in the negative controls (Sox10-wt; Fig. 2, D–G, upper panels). Searching for NC-derived cells, four thymi from Sox10-Cre Rosa-YFP mice were analyzed in parallel. As illustrated in one flow cytometric example (Fig. 2, D–G, lower panels), high YFP-labeling frequencies (70–80%) were found in NC-Mes (Fig. 2F). In contrast, YFP labeling was infrequent in TEC (~10% in Fig. 2, E and G), and absent in endothelium (Fig. 2D). Similar proportions of YFP<sup>+</sup> cells among stromal subsets were found in four mice of each genotype (data are summarized in Fig. 3).

Lack of endothelial labeling is consistent with a mesodermal origin of these cells that is unrelated to NC. The unexpected finding that some Sox10-Cre-mediated labeling occurred in TEC prompted further analyses of endogenous *Sox10* expression in TEC and NC-Mes from normal mice at fetal, newborn mice, and adult ages (Fig. 2H). Consistent with mesenchymal expression of *Sox10* only in premigratory NC, no *Sox10* expression was detectable in thymic NC-Mes at any time point. In contrast, at low levels, *Sox10* expression was detectable in TEC in fetal day 16.5 and in newborn, but not in adult mice (Fig. 2H). Hence, within thymic mesenchyme, the restricted *Sox10* expression in the emerging NC allows fate mapping of the majority of the Ly51<sup>+</sup>G8.8<sup>-</sup> population to NC origin. In contrast, infrequent YFP labeling in TEC can be explained by expression of *Sox10* in a small subset of TEC during ontogeny, rather than by a NC origin of a TEC subset.

Although frequencies of YFP-labeled Ly51<sup>+</sup>G8.8<sup>-</sup> cells were high, not all cells in this population were YFP<sup>+</sup> (Figs. 2 and 3). To address whether YFP<sup>-</sup>Ly51<sup>+</sup>G8.8<sup>-</sup> and YFP<sup>+</sup>Ly51<sup>+</sup>G8.8<sup>-</sup> cells differed, these subpopulations (Fig. 3, E and F) and TEC (G8.8<sup>+</sup>) (Fig. 3G) were isolated from adult mice, and analyzed by RT-PCR for expression of *Fgf10* and *Scf*. These two growth factors were

**FIGURE 2.** Phenotypic identification of Sox10-Cre-marked mesenchymal cells in the adult thymus. *A–C*, Gradient-enriched stromal cell suspensions from 8-wk-old Sox10-Cre Rosa-YFP mice were stained according to established cell surface phenotypes using UEA-1, G8.8, Ly51, and CD31 markers. Viable (Sytox<sup>-</sup>), nonlymphoid (CD45<sup>-</sup>) cells were analyzed for mTEC and cTEC, mesenchymal cell (Mes), and endothelial cell phenotypes. Cells were first gated as UEA-1<sup>+</sup> or CD31<sup>+</sup> (i.e., UEA-1 and CD31 combined in one color) Ly51<sup>-</sup> (A, gate R1), or UEA-1<sup>-</sup>CD31<sup>-</sup>Ly51<sup>+</sup> (A, gate R2). Endothelial cells were identified as CD31<sup>+</sup>Ly51<sup>-</sup>G8.8<sup>-</sup> (B, left gate), mTEC were recognized as UEA-1<sup>+</sup>Ly51<sup>-</sup>G8.8<sup>+</sup>CD31<sup>-</sup> (B, right gate), and the UEA-1<sup>-</sup>CD31<sup>-</sup>Ly51<sup>+</sup> population was further separated into G8.8<sup>-</sup> mesenchymal cells (C, left gate) and G8.8<sup>+</sup> cTEC (C, right gate). *D–G*, YFP expression was analyzed on endothelium (D), mTEC (E), NC-Mes (F), and cTEC (G). This analysis was made in parallel in normal mice (Sox10-wt Rosa-wt) (*D–G*, top row), in germline-deleted mice (Sox10-wt Rosa-YFP) (*D–G*, middle row), and under conditions of NC fate mapping (Sox10-Cre Rosa-YFP) (*D–G*, bottom row). The vast majority of NC-Mes, but only few TEC and no endothelial cells were labeled by YFP. *H*, Cell sorter-purified total TEC (G8.8<sup>+</sup>) (left) and NC-Mes (Ly51<sup>+</sup>G8.8<sup>-</sup>) (right) were isolated from fetal day 16.5, newborn, and 8-wk-old mice, and were analyzed by RT-PCR for expression of endogenous Sox10 (top) and actin (bottom). cDNAs were titrated in 2-fold steps to allow relative comparison. Sox10 expression was undetectable at any of the analyzed time points in NC-Mes, but was found at low levels in fetal and newborn TEC. Positive and negative controls were total thymus cDNA (P) and water (N), respectively.



examined because they were previously recognized as markers of Ly51<sup>+</sup>G8.8<sup>-</sup> mesenchyme (22). Both *Fgf10* and *Scf* were strongly expressed in both subsets of Ly51<sup>+</sup>G8.8<sup>-</sup> cells and, to a lesser extent, in TEC. Hence, YFP<sup>-</sup> and YFP<sup>+</sup> subsets of Ly51<sup>+</sup>G8.8<sup>-</sup> cells both expressed mesenchymal markers. This suggests that NC-Mes are very frequently, but not completely YFP labeled by Sox10-Cre, and argues against subsets among Ly51<sup>+</sup>G8.8<sup>-</sup> cells with distinct origins. In further support of the notion of incomplete labeling, frequencies of YFP<sup>+</sup>Ly51<sup>+</sup>G8.8<sup>-</sup> cells were similar in fetal day 16.5 (mean YFP<sup>+</sup> = 73.2% ± 12.8% (1 SD) in *n* = 4 mice) and adult mice (Fig. 3C). This implies that the ratio of YFP<sup>+</sup> to YFP<sup>-</sup> cells is fixed early in ontogeny, and remains constant thereafter.

#### NC-derived mesenchymal cells colocalize with the entire thymus vasculature in adult mice

YFP expression was next used to analyze abundance and position of NC-Mes in the adult thymus. Because direct YFP fluorescence was very weak on thymus tissue sections, we could initially recognize only very few YFP<sup>+</sup> cells, a notion consistent with previous reports that failed to detect substantial contribution of NC to the adult thymus (14, 18, 19). However, when YFP expression was probed using an anti-GFP Ab that cross-reacts with YFP, thymus-wide YFP protein expression became apparent (Fig. 4A). This YFP expression was specific for Sox10-Cre Rosa-YFP mice (Fig. 4B), as shown by lack of YFP staining in Sox10-wt control mice (Fig. 4C). On the sectional surface of two entire thymus lobes, YFP<sup>+</sup> cells were found in, from the outside to the inside, the capsule, scattered throughout the cortex, at the corticomedullary junction and in the medulla (Fig. 4A).

To characterize the nature of the YFP<sup>+</sup> structures within the thymus, sections were stained simultaneously for YFP, CD31, and keratin expression. In line with the flow cytometry data (Figs. 2

and 3), YFP expression was found mutually exclusive with keratin (Fig. 4G). In contrast, there was a remarkable colocalization of YFP<sup>+</sup> cells with the thymus vasculature, delineated by CD31 expression (Fig. 4F). Localization of YFP<sup>+</sup> cells in or close to the CD31<sup>+</sup> vasculature was observed not only for the large vessels in the medulla and at the corticomedullary junction, mostly venules and arterioles (34, 35), but also for the fine network of capillaries in the cortex (see below).

#### NC-Mes are $\alpha$ SMA<sup>+</sup> pericytes surrounding large blood vessels in the medulla and at the corticomedullary junction

To identify the vessel-associated cell types that were labeled by YFP, thymus sections were analyzed by three-color immunofluorescence for expression of YFP, CD31, and the pericyte marker,  $\alpha$ SMA. In large vessels located in the medulla and at the corticomedullary junction, an innermost layer of CD31<sup>+</sup> endothelial cells was tightly surrounded by a layer of YFP<sup>+</sup> cells (Fig. 5, A and D). Pericytes surrounding the endothelial layer were identified as CD31<sup>-</sup> $\alpha$ SMA<sup>+</sup> cells (Fig. 5, B and E). The perivascular position of YFP<sup>+</sup> cells strongly suggested that NC-Mes were identical with pericytes (Fig. 5, A–C). Indeed, confocal overlays demonstrated colocalization of YFP and  $\alpha$ SMA at the single cell level (Fig. 5F).

Next, expression of genes characteristic for perivascular mesenchyme was analyzed by RT-PCR in cell sorter-purified adult thymus stromal cells. TEC were collectively sorted as G8.8<sup>+</sup> cells (Fig. 5J), and compared with Ly51<sup>+</sup>G8.8<sup>-</sup> NC-Mes (Fig. 5K), and with CD31<sup>+</sup>Ly51<sup>-</sup>G8.8<sup>-</sup> endothelial cells (Fig. 5L). To verify the purity of these stromal cell preparations, the templates were analyzed for *Foxn1* expression that was, as expected, restricted to the TEC subset. In further support of the notion that NC-Mes correspond to pericytes, NC-Mes expressed  $\alpha$ SMA mRNA (Fig. 5K). In contrast,  $\alpha$ SMA mRNA was not expressed in thymus endothelium (Fig. 5L). In TEC,  $\alpha$ SMA mRNA expression was detectable, but

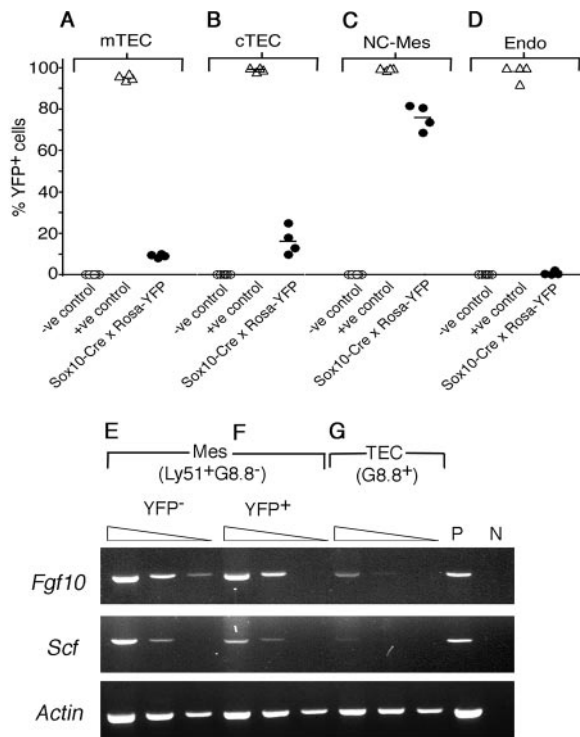


**FIGURE 3.** Contribution of YFP<sup>+</sup> cells to thymus stromal cell subsets. As described in Fig. 2, mTEC (A), cTEC (B), NC-Mes (C), and endothelial cells (Endo) (D) were analyzed by flow cytometry for the fraction of YFP-expressing cells. Genotypes analyzed were Sox10-wt Rosa-wt (negative control), germline-deleted Sox10-wt Rosa-YFP (positive control), and Sox10-Cre Rosa-YFP. Four mice per genotype were analyzed. Although greater 90% of the cells in all populations could, in principle, be labeled by YFP (see +ve controls), NC fate mapping selectively marked the vast majority of NC-Mes, but only few TEC and no endothelial cells. E–G, Cell sorter-purified YFP<sup>-</sup> (E) and YFP<sup>+</sup> (F) subsets of Ly51<sup>+</sup>G8.8<sup>-</sup> mesenchyme, and TEC (G8.8<sup>+</sup>) (G) from 12-wk-old Sox10-Cre Rosa-YFP mice were analyzed by RT-PCR for expression of *Fgf10* (top), *Scf* (middle), and *actin* (bottom). cDNAs were titrated in 5-fold steps to allow relative comparison. Positive and negative controls were total thymus cDNA (P) and water (N), respectively.

the expression was at least 5-fold lower than in NC-Mes, as shown by cDNA dilutions (Fig. 5, J and L). Finally, the smooth muscle marker *Cnn1* (Fig. 5K) was predominantly expressed in NC-Mes.

*NC-Mes are  $\alpha$ SMA<sup>+</sup> and  $\alpha$ SMA<sup>-</sup> pericytes surrounding capillary blood vessels in the cortex: evidence for smooth muscle cell heterogeneity in the thymus*

Blood vessels in the thymic cortex present as a dense capillary network of branching and anastomosing arcades (34). Histological examination of the cortex showed that YFP<sup>+</sup> cells were again closely associated with the vascular pattern revealed by CD31 staining (Fig. 4, A, B, D, and F). Three-color confocal analysis for expression of YFP, CD31, and  $\alpha$ SMA revealed three distinct cellular compositions of the vessel walls in cortical capillaries. In the first type, an inner layer of endothelium was covered by YFP<sup>+</sup> $\alpha$ SMA<sup>-</sup> cells, followed by YFP<sup>-</sup> $\alpha$ SMA<sup>+</sup> cells (Fig. 5G). The second type resembled the composition of large vessels in the medulla and at the corticomedullary junction, i.e., endothelium was surrounded by cells coexpressing  $\alpha$ SMA and YFP (Fig. 5H). The third type consisted only of endothelium surrounded by YFP<sup>+</sup> $\alpha$ SMA<sup>-</sup> cells (Fig. 5I). Hence, all capillaries were enclosed by NC-derived pericytes, some of which expressed  $\alpha$ SMA. Those that lacked expression of  $\alpha$ SMA could be encircled by other peri-

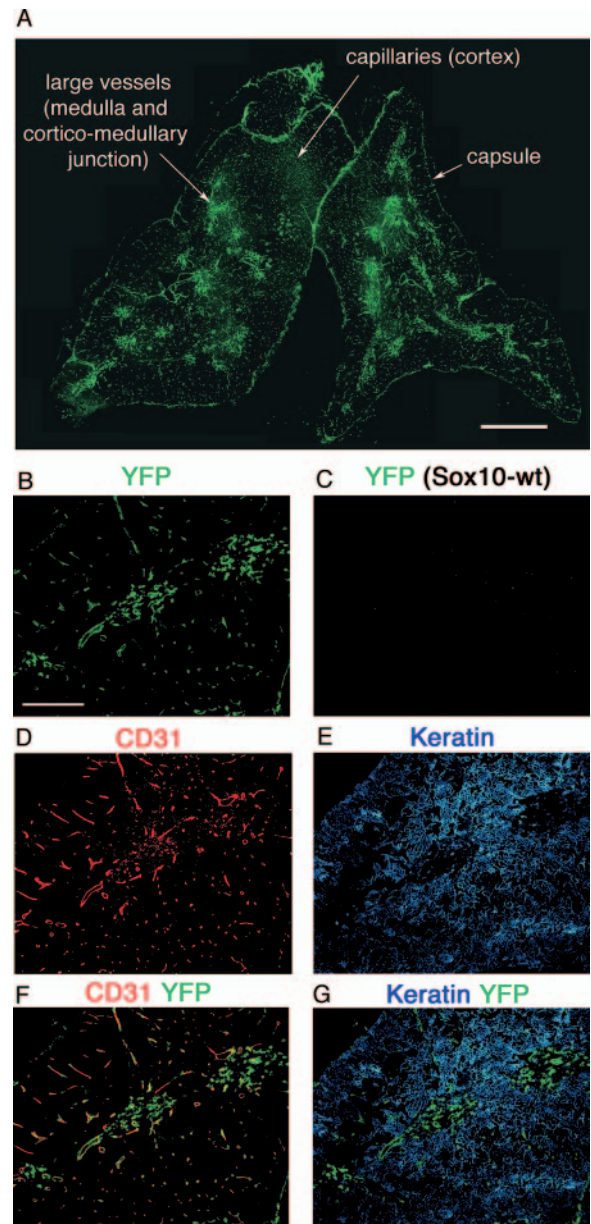


**FIGURE 4.** Blood vessel association of Sox10-Cre-marked cells in the adult thymus. A, Two entire thymus lobes from an 8-wk-old Sox10-Cre Rosa-YFP mouse were stained by anti-GFP Ab, cross-reacting with YFP, to visualize thymus-wide YFP protein expression. YFP<sup>+</sup> cells were present as part of the capsule, scattered throughout the cortex, at the corticomedullary junction and in the medulla. B–G, Sections from Sox10-Cre Rosa-YFP (B and D–G) and Sox10-wt Rosa-wt (Sox10-wt; C) were analyzed for expression of YFP (anti-GFP Ab) (B and C), CD31 (D), pan-cytokeratin (keratin; E), CD31 plus YFP (F), and keratin plus YFP (G). Comparison of Sox10-Cre Rosa-YFP (B) and Sox10-wt (C) demonstrates the specificity of the anti-YFP staining. YFP expression colocalized with the thymus vasculature, delineated by CD31 expression (F), and was mutually exclusive with keratin (G). Scale bar in A corresponds to 1 mm. Scale bar in B corresponds to 300  $\mu$ m, and applies to B–G.

cytes of non-NC origin (YFP<sup>-</sup> $\alpha$ SMA<sup>+</sup>). These data demonstrate considerable smooth muscle cell heterogeneity in thymus capillaries.

Finally, it was of interest to determine whether YFP<sup>-</sup> and YFP<sup>+</sup> subsets of Ly51<sup>+</sup>G8.8<sup>-</sup> cells showed a different distribution in the thymus. To this end, thymus sections from Sox10-Cre Rosa-YFP

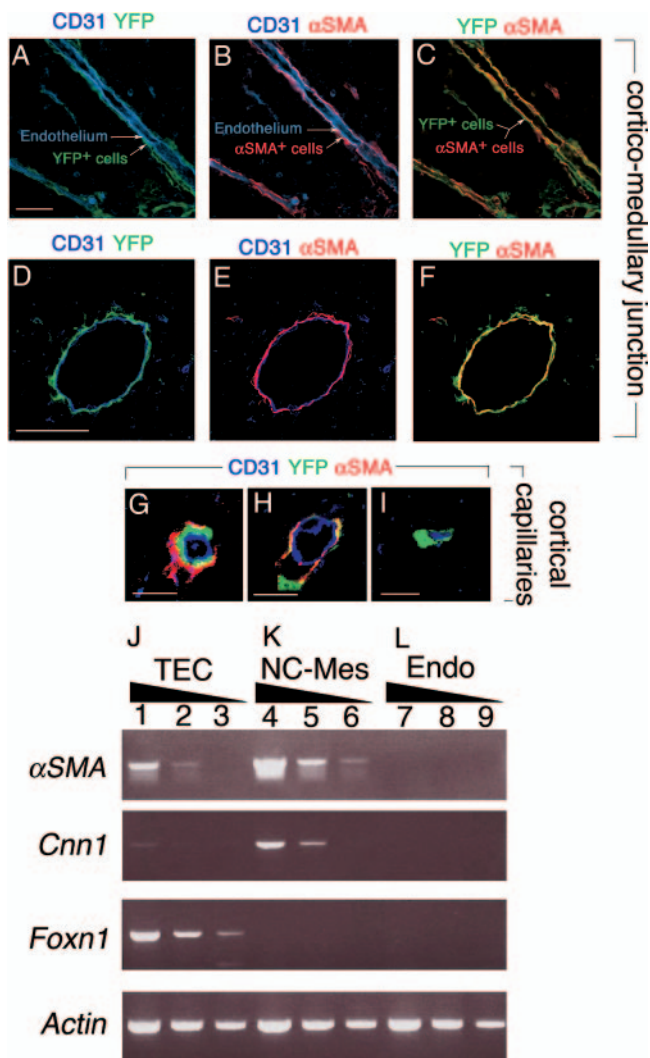


**FIGURE 5.** NC-derived cells contribute thymus-wide to perivascular mesenchyme. *A–F*, Thymus sections from an 8-wk-old Sox10-Cre Rosa-YFP mouse were analyzed by three-color immunofluorescence for expression of CD31 vs YFP (*A* and *D*), CD31 vs αSMA (*B* and *E*), and YFP vs αSMA (*C* and *F*). In large vessels in the medulla and at the corticom-edullary junction, the CD31<sup>+</sup> endothelial cell layer was covered by a layer of YFP<sup>+</sup> cells (*A* and *D*). Pericytes were identified as CD31<sup>-</sup>αSMA<sup>+</sup> cells (*B* and *E*). Confocal overlays revealed colocalization of YFP and αSMA (*F*). *G–I*, Three-color immunofluorescence analysis of cortical capillaries for expression of CD31, YFP, and αSMA. Three types of vessel wall configurations were observed, as follows: 1) an inner layer of endothelium covered by YFP<sup>+</sup>αSMA<sup>-</sup> cells, followed by YFP<sup>-</sup>αSMA<sup>+</sup> cells (*G*); 2) endothelium surrounded by cells coexpressing αSMA and YFP (*H*); and 3) endothelium surrounded by YFP<sup>+</sup>αSMA<sup>-</sup> cells (*I*). These data suggest smooth muscle cell heterogeneity in thymus capillaries. Scale bars correspond to 50 μm (*A*), 40 μm (*D*), 7 μm (*G*), 11 μm (*H*), and 9 μm (*I*). *J–L*, RT-PCR analysis for expression of pericyte-specific genes in cell sorter-purified adult TEC (G8.8<sup>+</sup>) (*J*), NC-Mes (Ly51<sup>+</sup>G8.8<sup>-</sup>) (*K*), and endothelial cells (CD31<sup>+</sup>Ly51<sup>-</sup>G8.8<sup>-</sup>) (*L*). cDNAs were analyzed for the pericyte markers αSMA and *Cnn1*, for the TEC-specific gene *Foxn1*, and were normalized for *actin* expression. cDNAs were titrated in 5-fold steps to allow relative comparisons.

mice were stained by three-color immunofluorescence for expression of Ly51, YFP, and CD31 (Fig. 6, *A* and *B*). YFP<sup>+</sup> pericytes were again surrounding CD31<sup>+</sup> endothelial cells (Fig. 6*A*). Unexpectedly, there was, with the exception of some Ly51<sup>+</sup>YFP<sup>+</sup> cortical cells, presumably representing the few YFP<sup>+</sup> cTEC (Fig. 2),

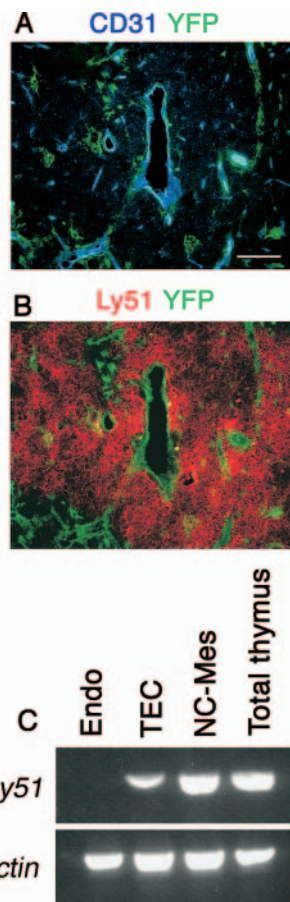


**FIGURE 6.** Analysis of Ly51 expression in thymic mesenchyme by histology and by RT-PCR. *A* and *B*, Thymus sections from an 8-wk-old Sox10-Cre Rosa-YFP mouse were analyzed by three-color immunofluorescence for expression of CD31, YFP, and Ly51. CD31 vs YFP, and Ly51 vs YFP are shown in *A* and *B*, respectively. Most YFP<sup>+</sup> cells lacked detectable Ly51 expression by immunofluorescence analysis on tissue sections. *C*, RT-PCR analysis for expression of *Ly51* mRNA in total thymus, and in cell sorter-purified adult thymic stromal populations (endothelial cells (CD31<sup>+</sup>Ly51<sup>-</sup>G8.8<sup>-</sup>), TEC (G8.8<sup>+</sup>), and NC-Mes (Ly51<sup>+</sup>G8.8<sup>-</sup>)). *Actin* expression was analyzed as positive control. cDNA templates were identical with those titrated in Fig. 5. Scale bar (*A*) corresponds to 100 μm.

no or very little colocalization of Ly51 with YFP staining (Fig. 6*B*). This raised the possibility that the Ly51<sup>+</sup> phenotype of NC-Mes reflected passive acquisition of the Ly51 molecule from surrounding cells. However, RT-PCR analysis clearly demonstrated cell-intrinsic expression of *Ly51* mRNA in NC-Mes (Fig. 6*C*). Hence, Ly51<sup>+</sup>G8.8<sup>-</sup> is a reliable phenotype by flow cytometry, but Ly51 staining cannot be used to detect this mesenchymal cell type on tissue sections. By histology, Ly51<sup>+</sup> cells in the cortex appear to be mostly G8.8<sup>+</sup>keratin<sup>+</sup> cTEC (data not shown). The bases for this discrepancy between Ly51 epitope detection by flow cytometry vs histology remain to be determined.

## Discussion

There is strong evidence for crucial functions of NC-derived mesenchyme in growth and differentiation of thymus epithelium during thymus organogenesis (for a recent analysis and further references, see Ref. 36). The contact between NC-Mes and TEC, as well as the significant structural contribution of NC-Mes to embryonic and fetal thymus stages (18, 19), raised the question of whether NC derivatives persist in the adult thymus and, if so, how such derivatives contribute to thymus function (9, 14, 15). Several

recent studies, also based on Cre-driven fate mapping, concluded that there is very little, if any, contribution of NC to the adult thymus (14, 18, 19). Collectively, the evidence demonstrated that NC is important during thymus development, but its role was considered to be limited to early stages (reviewed in Refs. 9 and 15).

We have readdressed this question in this study by systematically dissecting epithelial and mesenchymal stromal populations in the adult thymus for Sox10-Cre-driven, permanent YFP expression. Ideally, Cre-mediated fate mapping requires a gene locus that is expressed early and ubiquitously in the source population, but is later turned off in mature progeny. *Sox10* satisfies these criteria for the NC because its expression is restricted to the emerging NC before the diversification of its derivatives (26, 27). Importantly, *Sox10* expression was undetectable by RT-PCR in thymic NC-Mes at all fetal and adult stages analyzed. We conclude that the high frequency of YFP<sup>+</sup>Ly51<sup>+</sup>G8.8<sup>-</sup> mesenchymal cells reflects the NC origin of these cells rather than de novo expression of Cre in these cells.

Given that *Sox10* expression marks NC derivatives, it was surprising to find a low, but reproducible number of YFP<sup>+</sup> TEC in Sox10-Cre × Rosa-YFP mice (Figs. 2 and 3). This might suggest that the majority of YFP<sup>-</sup> and the minority of YFP<sup>+</sup> TEC have distinct origins, e.g., endoderm vs NC. However, *Sox10* expression was revealed by RT-PCR analysis in TEC isolated from fetal (day 16.5) and newborn thymi (Fig. 2). Activation of YFP expression in rare TEC was therefore not an artifact of the Sox10 BAC transgene in Sox10-Cre × Rosa-YFP mice because the endogenous *Sox10* gene is expressed in TEC at mid to end gestation. In this case, conclusions on lineage origins are precluded by expression of Cre in mature cells rather than in the originating progenitors.

The pattern of YFP-marked cells in the embryo was fully consistent with former reports showing NC-derived mesenchyme encapsulating the developing thymus (4, 18, 19) (Fig. 1). In similar lineage-tracing experiment using other NC marker genes (*Wnt1-Cre* (14, 18) and *P0-Cre* (19)), others also searched for Cre-marked progeny in the adult thymus. In all three cases, Rosa-LacZ was used as the reporter to reveal Cre activity. Marker detection in thymus stromal cells varies considerably depending on the marker used. For instance, *Foxn1-Gfp* (25) expression includes more TEC compared with a *Foxn1-LacZ* reporter (37). A further example is the Notch ligand *Delta-like-1* that appears more widely expressed in diverse stromal cells based on RT-PCR than in tissue sections based on *Delta-like-1-LacZ* reporter mice (A. Gossler and H.-R. Rodewald laboratories, unpublished observation). In this study, we searched for YFP expression by flow cytometric analysis, which has the added value of permitting the simultaneous analysis of several stromal cell phenotypes (Fig. 2). For the in situ location of YFP<sup>+</sup> cells, it was key to visualize YFP-expressing stromal cells on tissue sections using an anti-YFP Ab. This staining specifically identified a widely distributed cell population in Sox10-Cre × Rosa-YFP, but not in negative control thymi (Fig. 4). It is likely that both *Wnt1-Cre* and *P0-Cre* might yield a similar extent and specificity of labeling in thymic stromal cells when used in combination with Rosa-YFP, followed by Ab detection.

The cell type that was predominantly marked by its NC past, and that we now refer to as NC-Mes, has previously been identified by phenotype and by genetic complementation as a *Foxn1*-independent, mesenchymal thymic stromal population (22). These cells express growth factors such as *Scf* and *Fgfs*, which act on thymocytes and TEC, respectively. The original designation, cortical mesenchyme, was based on flow cytometric expression of the cortical marker Ly51 (22). However, because Ly51 is also expressed on cortical TEC (33), and Ly51 expression does not aid in localization of NC-Mes in the thymus (Fig. 6), the position and putative

function of these cells remained unknown. We have now identified these mesenchymal cells as the elusive NC-derived cells in the adult murine thymus. Remarkably, NC-Mes represent pericytes surrounding the endothelial layer of the vasculature, and by doing so they are spread virtually across the entire adult thymus (Fig. 4). A contribution of NC to perivascular mesenchyme was noted earlier by Le Douarin and Jotereau (4) for the developing chick thymus, but, to our knowledge, this link has not been reported for an adult thymus. There is also a precedent for NC-derived perivascular mesenchyme in other tissues. In the chicken embryo, NC contributes pericytes and smooth muscle cells, but not endothelium, to the aortic arch-derived vessels of the face and forebrain (28). Pericytes in other parts of the body are not NC derived. This implies directly that the thymic vasculature is part of the aortic arch-derived vessel network, and that this hallmark is retained in the adult thymus.

Thymic mesenchymal cells have been characterized before using specific markers, ER-TR7 and MTS15. These reagents have largely overlapping staining patterns that include structures in the capsule, the septae, thymic fibroblasts, and notably vessel-associated pericytes (16, 17). The majority of the MTS15<sup>+</sup> population also expresses Ly51 (17), and we show in this study that most Ly51<sup>+</sup> mesenchymal cells are of NC origin. Hence, NC-Mes represent a distinct mesenchymal cell type that is phenotypically included in populations marked by previously used reagents. However, NC-Mes differ from other thymic mesenchymal cells by their NC origin. Recent grafting experiments revealed that thymic mesenchymal cells, including those with a NC-Mes phenotype, could be largely replaced from nonthymic sources, at least when the thymus was placed under the kidney capsule (13). In our hands, we find only a low fraction of YFP-negative Ly51<sup>+</sup>G8.8<sup>-</sup> mesenchymal cells in adult mice, suggesting little or slow replacement of pericytes from outside of the normal adult thymus. It remains to be determined whether this also holds true for an aged thymus. Finally, a prominent marker of mesenchyme surrounding the embryonic thymus is the  $\alpha$ -subunit of the platelet-derived growth factor receptor (*Pdgfr*)  $\alpha$  (13). Adult NC-Mes lacked *Pdgfr* $\alpha$ , but expressed *Pdgfr* $\beta$  (data not shown), which is consistent with a previously reported pericyte phenotype in the adult thymus (38).

The finding that NC derivatives reside as pericytes in the adult thymus raises the possibility that NC-Mes also play a role in adult thymus function. The thymus appears highly selective in accepting blood-borne progenitors for entry, and in the gated export of self-tolerant mature T cells. This ability of the thymus to exclude virtually all nonpermissive cells may be related to the postulated blood-thymus barrier (34, 35). However, the blood-thymus barrier is poorly defined at a functional level, and it is not known how privileged entry and exit events are regulated. As a thymus-wide element of the perivascular space (35, 38), NC-Mes might contribute to specific functions of the blood-thymus barrier in the adult thymus, and may be part of the microenvironment that receives and supports recent thymic immigrants. The ontogenetic, phenotypic, and positional definition of NC-Mes as a distinct perivascular mesenchymal cell population might therefore provide a basis on which to address properties of the endothelial-epithelial barrier in the adult thymus.

## Acknowledgments

The confocal analyses were done at the Nikon Imaging Center at the University of Heidelberg using a Nikon C1si instrument. We thank Carolin Lauffle for technical assistance, Dennis Pfaff for help at the confocal microscope, Iris Helfrich for advice on pericyte staining, Thomas Wirth as a fruitful seminar host, and Hellmut Augustin and Hans Jorg Fehling for discussions.

## Disclosures

The authors have no financial conflict of interest.

## References

- Etchevers, H. C., G. Couly, and N. M. Le Douarin. 2002. Morphogenesis of the branchial vascular sector. *Trends Cardiovasc. Med.* 12: 299–304.
- Matsuoka, T., P. E. Ahlberg, N. Kessaris, P. Iannarelli, U. Denhehy, W. D. Richardson, A. P. McMahon, and G. Koentges. 2005. Neural crest origins of the neck and shoulder. *Nature* 436: 347–355.
- Brown, C. B., and H. S. Baldwin. 2006. Neural crest contribution to the cardiovascular system. *Adv. Exp. Med. Biol.* 589: 134–154.
- Le Douarin, N. M., and F. V. Jotereau. 1975. Tracing of cells of the avian thymus through embryonic life in interspecific chimeras. *J. Exp. Med.* 142: 17–40.
- Bockman, D. E., and M. L. Kirby. 1984. Dependence of thymus development on derivatives of the neural crest. *Science* 223: 498–500.
- Manley, N. R. 2000. Thymus organogenesis and molecular mechanisms of thymic epithelial cell differentiation. *Semin. Immunol.* 12: 421–428.
- Anderson, G., and E. J. Jenkinson. 2001. Lymphostromal interactions in thymic development and function. *Nat. Rev. Immunol.* 1: 31–40.
- Blackburn, C. C., and N. R. Manley. 2004. Developing a new paradigm for thymus organogenesis. *Nat. Rev. Immunol.* 4: 278–289.
- Rodewald, H.-R. 2007. Thymus organogenesis. *Annu. Rev. Immunol.* 26: 355–388. doi: 10.1146/annurev.immunol.26.021607.090408.
- Anderson, G., E. J. Jenkinson, N. C. Moore, and J. J. Owen. 1993. MHC class II-positive epithelium and mesenchyme cells are both required for T-cell development in the thymus. *Nature* 362: 70–73.
- Shinohara, T., and T. Honjo. 1996. Epidermal growth factor can replace thymic mesenchyme in induction of embryonic thymus morphogenesis in vitro. *Eur. J. Immunol.* 26: 747–752.
- Suniar, R. K., E. J. Jenkinson, and J. J. Owen. 2000. An essential role for thymic mesenchyme in early T cell development. *J. Exp. Med.* 191: 1051–1056.
- Jenkinson, W. E., S. W. Rossi, S. M. Parnell, E. J. Jenkinson, and G. Anderson. 2007. PDGFR $\alpha$ -expressing mesenchyme regulates thymus growth and the availability of intrathymic niches. *Blood* 109: 954–960.
- Petrie, H. T. 2002. Role of thymic organ structure and stromal composition in steady-state postnatal T-cell production. *Immunol. Rev.* 189: 8–19.
- Manley, N. R., and C. C. Blackburn. 2003. A developmental look at thymus organogenesis: where do the non-hematopoietic cells in the thymus come from? *Curr. Opin. Immunol.* 15: 225–232.
- Van Vliet, E., M. Melis, J. M. Foidart, and W. Van Ewijk. 1986. Reticular fibroblasts in peripheral lymphoid organs identified by a monoclonal antibody. *J. Histochem. Cytochem.* 34: 883–890.
- Gray, D. H., D. Tull, T. Ueno, N. Seach, B. J. Classon, A. Chidgey, M. J. McConville, and R. L. Boyd. 2007. A unique thymic fibroblast population revealed by the monoclonal antibody MTS-15. *J. Immunol.* 178: 4956–4965.
- Jiang, X., D. H. Rowitch, P. Soriano, A. P. McMahon, and H. M. Sucov. 2000. Fate of the mammalian cardiac neural crest. *Development* 127: 1607–1616.
- Yamazaki, H., E. Sakata, T. Yamane, A. Yanagisawa, K. Abe, K. Yamamura, S. Hayashi, and T. Kunisada. 2005. Presence and distribution of neural crest-derived cells in the murine developing thymus and their potential for differentiation. *Int. Immunol.* 17: 549–558.
- Blackburn, C. C., C. L. Augustine, R. Li, R. P. Harvey, M. A. Malin, R. L. Boyd, J. F. Miller, and G. Morahan. 1996. The *nu* gene acts cell-autonomously and is required for differentiation of thymic epithelial progenitors. *Proc. Natl. Acad. Sci. USA* 93: 5742–5746.
- Martinic, M. M., T. Rulicke, A. Althage, B. Odermatt, M. Hochli, A. Lamarre, T. Dumrese, D. E. Speiser, D. Kyburz, H. Hengartner, and R. M. Zinkernagel. 2003. Efficient T cell repertoire selection in tetraparental chimeric mice independent of thymic epithelial MHC. *Proc. Natl. Acad. Sci. USA* 100: 1861–1866.
- Muller, S. M., G. Terszowski, C. Blum, C. Haller, V. Anquez, S. Kuschert, P. Carmeliet, H. G. Augustin, and H. R. Rodewald. 2005. Gene targeting of VEGF-A in thymus epithelium disrupts thymus blood vessel architecture. *Proc. Natl. Acad. Sci. USA* 102: 10587–10592.
- Chidgey, A. P., and R. L. Boyd. 2006. Stemming the tide of thymic aging. *Nat. Immunol.* 7: 1013–1016.
- Srinivas, S., T. Watanabe, C. S. Lin, C. M. William, Y. Tanabe, T. M. Jessell, and F. Costantini. 2001. Cre reporter strains produced by targeted insertion of EYFP and ECFP into the ROSA26 locus. *BMC Dev. Biol.* 1: 4.
- Terszowski, G., S. M. Muller, C. C. Bleul, C. Blum, R. Schirmbeck, J. Reimann, L. D. Pasquier, T. Amagai, T. Boehm, and H. R. Rodewald. 2006. Evidence for a functional second thymus in mice. *Science* 312: 284–287.
- Britsch, S., D. E. Goerich, D. Riethmacher, R. I. Peirano, M. Rossner, K. A. Nave, B. Birchmeier, and M. Wegner. 2001. The transcription factor Sox10 is a key regulator of peripheral glial development. *Genes Dev.* 15: 66–78.
- Stolt, C. C., S. Rehberg, M. Ader, P. Lommes, D. Riethmacher, M. Schachner, U. Bartsch, and M. Wegner. 2002. Terminal differentiation of myelin-forming oligodendrocytes depends on the transcription factor Sox10. *Genes Dev.* 16: 165–170.
- Etchevers, H. C., C. Vincent, N. M. Le Douarin, and G. F. Couly. 2001. The cephalic neural crest provides pericytes and smooth muscle cells to all blood vessels of the face and forebrain. *Development* 128: 1059–1068.
- Gordon, J., A. R. Bennett, C. C. Blackburn, and N. R. Manley. 2001. Gcm2 and Foxn1 mark early parathyroid- and thymus-specific domains in the developing third pharyngeal pouch. *Mech. Dev.* 103: 141–143.
- Farr, A. G., and S. K. Anderson. 1985. Epithelial heterogeneity in the murine thymus: fucose-specific lectins bind medullary epithelial cells. *J. Immunol.* 134: 2971–2977.
- Farr, A., A. Nelson, J. Truex, and S. Hosier. 1991. Epithelial heterogeneity in the murine thymus: a cell surface glycoprotein expressed by subcapsular and medullary epithelium. *J. Histochem. Cytochem.* 39: 645–653.
- Derbinski, J., A. Schulte, B. Kyewski, and L. Klein. 2001. Promiscuous gene expression in medullary thymic epithelial cells mirrors the peripheral self. *Nat. Immunol.* 2: 1032–1039.
- Gray, D. H., A. P. Chidgey, and R. L. Boyd. 2002. Analysis of thymic stromal cell populations using flow cytometry. *J. Immunol. Methods* 260: 15–28.
- Raviola, E., and M. J. Karnovsky. 1972. Evidence for a blood-thymus barrier using electron-opaque tracers. *J. Exp. Med.* 136: 466–498.
- Kato, S. 1997. Thymic microvascular system. *Microsc. Res. Tech.* 38: 287–299.
- Itoi, M., N. Tsukamoto, H. Yoshida, and T. Amagai. 2007. Mesenchymal cells are required for functional development of thymic epithelial cells. *Int. Immunol.* 19: 953–964.
- Nehls, M., B. Kyewski, M. Messlerle, R. Waldschutz, K. Schuddekopf, A. J. Smith, and T. Boehm. 1996. Two genetically separable steps in the differentiation of thymic epithelium. *Science* 272: 886–889.
- Mori, K., M. Itoi, N. Tsukamoto, H. Kubo, and T. Amagai. 2007. The perivascular space as a path of hematopoietic progenitor cells and mature T cells between the blood circulation and the thymic parenchyma. *Int. Immunol.* 19: 745–753.